Nano World Journal

https://doi.org/10.17756/nwj.2022-s1-019

Research Article

Open Access

Unsteady MHD flow of Tangent Hyperbolic Nanofluid over an Inclined Stretching Sheet and Heat Transfer Analysis

Kavita Jat and Kalpna Sharma*

Department of Mathematics and Statistics, Manipal University Jaipur, Jaipur, Rajasthan, India

***Correspondence to:**
Kalpna Sharma

Department of Mathematics and Statistics
Manipal University Jaipur, Jaipur
Rajasthan, India

E-mail: kalp_aali@yahoo.co.in

Received: August 23, 2022
Accepted: October 24, 2022
Published: October 27, 2022

Citation: Jat K, Sharma K. 2022. Unsteady MHD flow of Tangent Hyperbolic Nanofluid over an Inclined Stretching Sheet and Heat Transfer Analysis. *NanoWorld J* 8(S1): S104-S110.

Published by United Scientific Group

Abstract

This paper explores the time dependent magnetohydrodynamic (MHD) flow of tangent hyperbolic nanofluid with flucating flow properties over an inclined stretched sheet in the presence of a heat source. The governing nonlinear partial differential equations of current flow analysis are equations of continuity, momentum, temperature, and concentration those are converted into dimensionless form and numerically solved using the shooting technique and the bvp4c solver approach. Under limited conditions, numerical findings were compared to previously reported results. Non-dimensional profiles were depicted graphically related to velocity, temperature, and concentration. Results show that for increased values of the power-law index and Weissenberg number cause a rise in the temperature and concentration profiles, while a drop in the velocity profile. In the current study, the Weissenberg number and power law index parameters enhances skin friction and reduced heat and mass transfer rate.

Keywords

Magnetohydrodynamics, Tangent hyperbolic nanofluid, Heat source, Inclined stretching sheet, bvp4c techinque

Abbreviation

Ha: Hartmann number; **P**: Porous medium parameter; $\mathbf{A}^*$: Unsteadiness parameter; $\mathbf{Gr}_x$: Local Grashof number; $\mathbf{Gm}_x$: Local Grashof number for mass; **Pr**: Prandtl number; **Ec**: Eckert number; **N**: Radiation parameter; $\mathbf{f}_w$: Suction/ injection parameter; $\mathbf{T}_w$: Temperature of sheet at wall (K); $\mathbf{T}_\infty$: Temperature far from the sheet (K); **u, v**: Velocity components (LT^{-1}); $\mathbf{v}_w(\mathbf{t})$: Velocity of the mass transfer (LT^{-1}); $\boldsymbol{u_w(x, t)}$: Velocity of the stretching sheet (LT^{-1}); **g**: Earth's gravity (LT^{-2}); **x, y:** Cartesian coordinates; **Sc**: Schmidt number; **Cr**: Chemical reaction parameter; ***F***: Force applied along x – axis ($ML^{-1}T^{-2}$); ***t***: Time(T^{-1}); $\mathbf{C}_{fx}$: Skin frication coefficient; ***b***: Constants; c: Stretching rate (T^{-1}); $\mathbf{C}_p$: Constant heat capacity pressure ($L^2T^{-2}K^{-1}$); $\mathbf{H}_0$: Magnetic field strength (LA); **K**: Permeability factor; $\mathbf{K}_1$: Rate of chemical reaction; $\mathbf{C}_\infty$: Concentration far from the sheet (ML^{-3}); $\mathbf{Nu}_x$: Nusselt number; **T**: Temperature of the fluid (K); $\mathbf{C}_w$: Concentration of fluid at the wall (ML^{-3}); **D**: Diffusion coefficient (L^2T^{-1}); $\mathbf{Re}_x$: Local Reynold number; $\mathbf{Sh}_x$**:** Local Sherwood number; **α**: Inclination angle; **γ**: Constant; **δ**: Heat generation/ absorption parameter; **ρ**: Fluid density (ML^{-3})**;** **σ**: Fluid electrical conductivity ($M^{-1}L^{-3}T^3A^2$); **υ**: Kinematic viscosity (L^2T^{-1}); **ψ**: Stream function; **κ**: Thermal conductivity; $\boldsymbol{\kappa}^*$: Mean absorption coefficient($L^{-1}TK^3$); $\mathbf{q}_r$: Radiation heat flux (ML^2T^{-3}) ; **η**: Similarity variable; **Δ**: Delta; $\boldsymbol{\beta}_t$: Thermal expansion coefficient (K^{-1}); $\boldsymbol{\beta}_c$: Solute expansion coefficient ($M^{-1}L^3$); $\boldsymbol{\tau}_w$: Shear stress ($ML^{-1}T^{-2}$); $\boldsymbol{\sigma}^*$: Stpheman Boltzman constant ($ML^2T^9K^{-1}$)

Introduction

The flow behaviour of non-Newtonian fluids has intrigued researchers and engineers during the last few decades. These rheological fluids, unlike Newtonian liquids, have been extensively used in a variety of engineering and operational industries. Biomechanics, polymer processing, food production, and increased oil recovery are some of these processes. Such fluids' rheological properties cannot be represented by a single constitutive equation. As a result, various constitutive equations have been described in the literature in order to predict the properties of fluid models subjected to non-Newtonian liquids. Among non-Newtonian fluid models, the tangent hyperbolic fluids model [1-3], is capable of anticipating shear thinning (Pseudo-plastic). It is a type of fluid that influences fluid resistance by having a high shear stress rate. Ketchup, watercolours, blood, nail polish, and whipped cream are examples of such fluids. Many number of academicians had published significant analyses fluid model of tangent hyperbolic fluid, while accounting for various flow phenomena. Khan et al. [4] investigated the formation of entropy in the radiative motion of a tangent hyperbolic nanofluid in the presence of activation energy and nonlinear mixed convection. Ullah et al. [5] and Waqas et al. [6] described MHD tangent hyperbolic nanofluid flow past a stretched sheet and riga plate respectively.

The greatest fascinating domain in public health is nanotechnology [7, 8]. This subject of study is deemed embryonic because to its breadth and advancement in micro technology. Numerous investigations have proven that heat transfer phenomena are a requirement for multi-scale buildings. Several experiments have been presented by researchers and engineers in order to increase the heat transfer rate. Nanoparticles are a blend of conventional fluids and microscopic nanoparticles that are evenly disseminated in a conventional fluids and exhibit outstanding heat transport qualities. Metals and their oxides of these nanoparticles are utilised to improve coefficients of convection and conduction, thermal conductivity, and heat exchange strategies described by Hakeem et al. [9] and Khan et al. [10]. It is thought to be enthralling research with fairly excellent output but at a lesser cost. Increasing heat transmission over short regions is a significant application of nanofluids. As a result, the irreversibility of the thermal system and the rate of entropy development both decrease. Modern advancements in electronics have enhanced electrical gadget functioning. Countless researchers are attempting to optimise these digital appliances due to the resource consumption connected with these items, which raises the heat flux dramatically. Thermal research looked at the disadvantages of heat flow rate management in digital equipment, such as burning, which limits the instrument's longevity and quality of improvement. Nowadays, investigators face a significant barrier in constructing an effective water - cooling model. Such type systems of cooling will regulate generation heat in order to keep electronic devices cold mentioned in [11]. Nanoparticles with a good thermal character and a moderate capacity ratio are used to improve heating processes. Researchers have given nanofluids high marks for their practical utility in biomedical and engineering applications. The development of nanofluids has proven to be substantial and beneficial in boosting heat transfer rate efficiency. Nanoparticles have gained respect in recent years as a result of their critical significance in industrial and biochemical engineering. The productivity of various organic solvents such as ethyl alcohol, freshwater, and lubricant have been adjusted for energy improvement were investigated [12, 13]. It should be emphasised that when heat fluxes are high, the system requires solvent freezing. The increase in virtue of thermal conductivity of fluid, due to its numerous areas of science and engineering, is a source of great interest for researchers.

The MHD boundary layer flow past an inclined extended sheet has fascinated the interest of many researchers in references [14-20] due to its meaningful applications in a wide range of various engineering and advanced manufacturing industries processes including such electrical power stations, wire drawing, magnetic resonance imaging, printer ink, synthetic fibers, polyethylene, and several others. Makinde et al. [14] investigated the MHD flow of a variable viscosity nanofluid over a radially expanding convective surface with radiative heat.

Over an inclined stretched sheet, we have examined the time-dependent MHD fluid motion of a tangent hyperbolic nanofluid with a heat generationobservation parameter. Also using the similarity transformation, the controlling nonlinear partial differential equations can be written as a set of non-dimensional ordinary differential equations. Afterwards, the nonlinear ordinary differential equations are computed numerically by the shooting approach after being converted. The MATLAB programme bvp4c was used to generate the numerical results. At last, we addressed how the non-dimensional governing factors affect the physical quantities of interest, including velocity, temperature, and concentration.

Problem Formulation

Consider the flow of a tangent hyperbolic nanofluid over a permeable inclined stretching sheet in a two-dimensional incompressible laminar boundary layer MHD that is not steady. The stretching sheet adds heat to the nanofluid, and the concentration of chemical species goes up and down at the same rate. It is assumed that density alternations caused by changes in temperature and concentration only affect the body force term, so changes in both concentration and temperature cause the buoyant strength. A homogeneous magnetic field is put on the surface of the extending sheet in the same direction as the surface. Also, it is assumed that in the flow there is a homogeneous first-order chemical reaction with heat radiation. It is assumed that the sheet's speed, $u_w(x,t)$, is in the same way as the force, F, which is acting along the x-axis, and that the mass transfer speed, $v_w(t)$, is parallel to the extended sheet. It is presumed that the temperature and concentration on the surface (wall) of the sheet are $T_w(x,t)$ and $C_w(x,t)$, respectively, and that the temperature and concentration far away from the sheet are T_∞ and C_∞, respectively. Also, it is commonly agreed that the outcome characterized by Fourier's law and Fick's law is bigger than the influence caused by Dufour and Soret. This means, impacts of

Dufour and Soret, are not taken into account. In general, it is accepted, both the heat conductivity and molecular diffusivity of a fluid are thought to change linearly as the temperature changes.

Based on the above assumptions and using the tangent hyperbolic fluid model [21], the governing partial differential equations for the present fluid model are:

$$\frac{\partial u}{\partial x}+\frac{\partial v}{\partial y}=0 \tag{1}$$

$$\frac{\partial u}{\partial t}+u\frac{\partial u}{\partial x}+v\frac{\partial u}{\partial y}=\upsilon\left[(1-n)\frac{\partial^2 u}{\partial y^2}+\sqrt{2}n\Gamma\frac{\partial u}{\partial y}\frac{\partial^2 u}{\partial y^2}\right]-\frac{\upsilon}{K}u-\frac{\sigma}{\rho}H_0^2u+g\beta_1(T-T_\infty)\cos(\alpha)+g\beta_c(C-C_\infty)\cos(\alpha) \tag{2}$$

$$\frac{\partial T}{\partial t}+u\frac{\partial T}{\partial x}+v\frac{\partial T}{\partial y}=\frac{1}{\rho c_p}\frac{\partial}{\partial y}\left(\kappa(T)\frac{\partial T}{\partial y}\right)-\frac{1}{\rho c_p}\frac{\partial q_r}{\partial y}+ \tag{3}$$

$$\frac{\mu}{\rho c_p}\left[(1-n)\left(\frac{\partial u}{\partial y}\right)^2+\frac{n\Gamma}{\sqrt{2}}\left(\frac{\partial u}{\partial y}\right)^3\right]+\frac{Q_0}{\rho c_p}(T-T_\infty)$$

$$\frac{\partial C}{\partial t}+u\frac{\partial C}{\partial x}+v\frac{\partial C}{\partial y}=-K_1(C-C_\infty)+\frac{\partial}{\partial y}\left(D(T)\frac{\partial C}{\partial y}\right) \tag{4}$$

where t represents time, u and v are velocity components in the x and y - directions, respectively, n is the power law fluid velocity index, $\Gamma>0$ is the time dependent material constant, and Q_0 is the heat absorption/observation coefficient.

$$\left.\begin{aligned}&u=u_w(x,t)=\frac{cx}{1-\gamma t},\\&v=v_w(t),\\&T=T_w(x,t),\\&C=C_w(x,t)\end{aligned}\right\}\ \text{at } y=0 \quad \text{and} \quad \left.\begin{aligned}&u\to 0,\\&T\to T_\infty,\\&C\to C_\infty\end{aligned}\right\}\ \text{as } y\to\infty \tag{5}$$

Boundary conditions are given by
where c denotes the opening/initial stretching rate, γ denotes a constant, and subscript w and ∞ denote the sheet and boundary layer edges (ambient conditions), respectively. Fluid suction velocity for flow, which is also named as wall

mass transfer velocity, is $v_w(t)=-\upsilon_0\sqrt{\frac{\upsilon c}{(1-\gamma t)}}$ and it is constant. υ_0 is also constant that characterizes transfer parameter for wall mass, with the means that when $\upsilon_0>0$ is suction, when $\upsilon_0=0$ is impermeability, and when $\upsilon_0<0$ is injection. The Rosseland's approximation q_r is used according to

$$T_w(x,t)=T_\infty+\frac{bx}{(1-\gamma t)^2} \quad \text{and} \quad C_w(x,t)=C_\infty+\frac{bx}{(1-\gamma t)^2} \tag{6}$$

Mukhopadhyay [22] in temperatue equation (3).
here, $b=0$ stands to the amount of enforced convection in the absence of buoyant force.

By introducing the dimensionless variables (7) into the partial differential equations (2)-(4), and (5), they are changed

$$\eta=\sqrt{\frac{c}{\upsilon(1-\gamma t)}}y,\quad \psi=\sqrt{\frac{\upsilon c}{(1-\gamma t)}}xf(\eta),\quad \theta=\frac{T-T_\infty}{T_w-T_\infty}\ \text{and}\ \phi=\frac{C-C_\infty}{C_w-C_\infty} \tag{7}$$

into ordinary differential equations:

where $\upsilon=\frac{\mu}{\rho}$ is the kinematic viscosity of the free stream, ψ is a stream function that defines the velocity components as $u=\frac{\partial\psi}{\partial y}=\frac{cx}{(1-\gamma t)}f'(\eta)$, $v=-\frac{\partial\psi}{\partial x}=-\sqrt{\frac{\upsilon c}{(1-\gamma t)}}f(\eta)$,

and fulfils the requirements of the continuity equation (1), $f(\eta)$ stands for suction and injection, η stands for the dimensionless spatial variable, $\theta(\eta)$ and $\phi(\eta)$ symbolize for the dimensionless temperature and concentration of the fluid, respectively.

The thermal conductivity $\kappa(T)$ of nano-fluid can gradually fluctuate with heat according to the function illustrated in (8), as suggested by Hunegnaw and Kishan [23] and Vajravelu [24]:

$$\kappa(T)=\kappa_\infty\left(1+\frac{\beta_1}{\Delta T}(T-T_\infty)\right) \tag{8}$$

Following Dimian and Hadhoda [25], and based on many similarities between mass transfer and heat transfer throughout the cooling phase, one can summarize diffusion coefficient $D(T)$ as an expression(linear) of temperature, as indicated in equation (9):

$$D(T)=D_\infty\left(1+\frac{\beta_2}{\Delta T}(T-T_\infty)\right) \tag{9}$$

Reduced system of equations is given by-

$$f'''=\frac{\frac{A^*}{2}\eta f''+\left(A^*+P+Ha\right)f'-ff''+(f')^2-Gr_x\theta-Gm_x\phi}{(1-n)+nWef''} \tag{10}$$

$$\theta''=\frac{-\beta_1(\theta')^2+Pr\left[\frac{A^*}{2}\eta\theta'+2A^*\theta+f'\theta-f\theta'-(1-n)Ec(f'')^2-\frac{n}{2}WeEc(f'')^3-\delta\theta\right]}{1+\beta_1\theta+\frac{4}{3}N} \tag{11}$$

$$\phi''=\frac{-\beta_2\theta'\phi'+Sc\left[2A^*\phi+\frac{A^*}{2}\eta\phi'+f'\phi-f\phi'+Cr\phi\right]}{1+\beta_2\theta} \tag{12}$$

with starting and boundary conditions which are given in dimensionless form by eq. (13).

$$\left.\begin{aligned}&f(0)=f_w\\&f'(0)=1\\&\theta(0)=1\\&\phi(0)=1\end{aligned}\right\}\ \text{at}\ \eta=0 \quad \text{and} \quad \left.\begin{aligned}&f'(\eta)\to 0\\&\theta(\eta)\to 0\\&\phi(\eta)\to 0\end{aligned}\right\}\ \text{at}\ \eta\to\infty \tag{13}$$

where $P=\frac{\upsilon(1-\gamma t)}{cK}$, $A^*=\frac{\gamma}{c}$, $Ha=\frac{\sigma B_0^2(1-\gamma t)}{\rho c}$, $Gr_x=\frac{g\beta_1 x(T_w-T_\infty)}{u_w^2}\cos(\alpha)$, $Sc=\frac{\upsilon}{D_\infty}$, $Pr=\frac{c_p\mu}{\kappa_\infty}$,
$Gm_x=\frac{g\beta_c x(C_w-C_\infty)}{u_w^2}$, $Cr=\frac{K_1(1-\gamma t)}{c}$, $Ec=\frac{u_w^2}{c_p(T_w-T_\infty)}$, $N=\frac{4\sigma^*T_\infty^3}{\kappa^*\kappa_\infty}$, $We=\Gamma\sqrt{\frac{2c^3}{(1-\gamma t)^3}}x$

and $\delta = \frac{Q_0}{\rho c_p}\frac{(1-\gamma t)}{c}$ are the unsteadiness parameter, porous medium parameter, Hartmaan number parameter, thermal Grashof number, Schmidt number, Prandtl number, solutal or concentration Grashof number, thermal radiation parameter, chemical reaction parameter, Eckert number, Weissenberg number and heat generation/absorption coefficient respectively.

It is also worth mentioning that the primary symbol signifying differentiation with regard to η variable that has no dimension in space. The fundamental and real engineering quantities of interest in this model are coefficient of skin friction (C_{fx}), Nusselt number (Nu_x), and Sherwood number (Sh_x), which are expressed as:

$$\frac{1}{2}C_{f_x}\sqrt{Re_x} = \left\{\frac{n}{2}We\left(f''\right)^2 + (1-n)f''\right\}, \frac{Nu_x}{\sqrt{Re_x}} = -\left(1+\frac{4}{3}N\right)\theta'(0) \text{ and } Sh_x\, Re_x^{-\frac{1}{2}} = -\phi'(0) \quad (14)$$

Results and Discussions

The present analysis is validated by comparing the results for coefficient of skin friction $f''(0)$, Nusselt number $-\grave{e}'(0)$, and the mass transfer $-\phi'(0)$ with those given by Mjankwi et al. [26], as featured in Table 2, and a near identical cooperation has been noted. Study's findings were disclosed in the form of tables and charts and explained in detail. Here, we share the findings from the research. The profiles of dimensionless velocities $f'(\eta)$, temperatures $\theta(\eta)$, and nanoparticle concentrations $\phi(\eta)$, and the surface friction coefficients $f''(0)$, Nusselt number $\theta'(0)$, and Sherwood number $\phi'(0)$ were analyzed as a function of some relevant parameters, with all other parameters held constant.

The Weissenberg number We is the ratio of the time takes for a fluid to relax to the viscous forces acting on it. Figures 1-3 depict the effects of We on $f'(\eta)$, $\phi(\eta)$ and $\phi(\eta)$, respectively. As can be seen, the fluid velocity drops and the temperature along with concentration profiles rise progressively with increasing values of We. The reason for this is that as We grows, the nanofluid's relaxation time also grows, or the nanofluid's thickness increases, creating more resistance in the flow field. In the boundary layer region, the tangent hyperbolic nano-

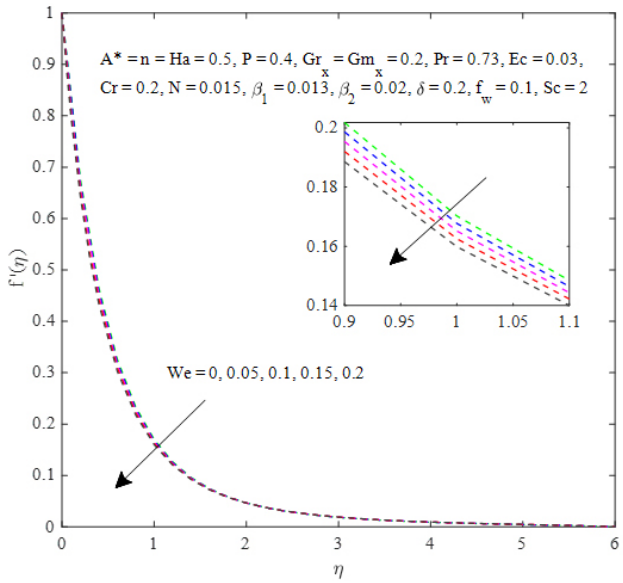

Figure 1: Velocity profile against We.

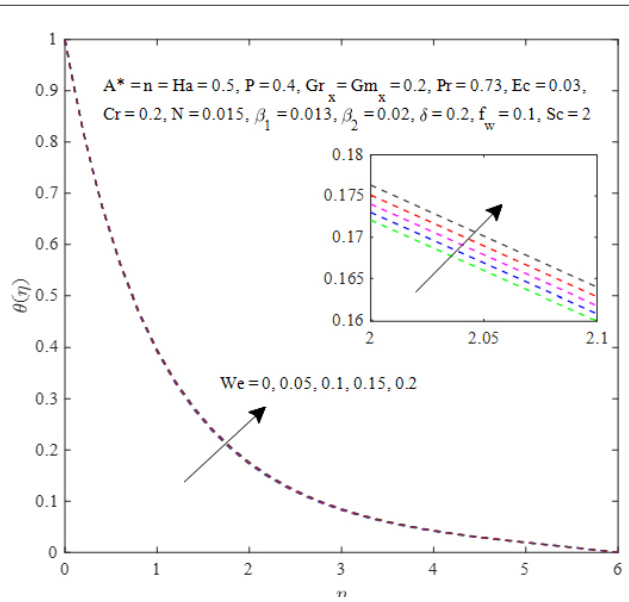

Figure 2: Temperature profile against We.

Table 2: Comparison of numerical values for coefficient of skin friction f"(0), Nusselt number-θ'(0) and -ϕ'(0) when Ec=0.03, Sc=2, β_2=0.01, P=Ha=0.5, n=We=δ=0,Pr= 0.72, N=0.0075 and f_w=Gr_x=Gm_x=Cr=0.1.

β_1	A^*	Mjankwi et al. [26]			Present Work		
		$f''(0)$	$-\theta'(0)$	$-\phi'(0)$	$f''(0)$	$-\theta'(0)$	$-\phi'(0)$
0.020	0.5	-1.5222	1.1281	2.1268	-1.522253	1.128119	2.126785
0.035	0.5	-1.5221	1.1167	2.1269	-1.522125	1.116689	2.126822
0.040	0.5	-1.5221	1.1129	2.1408	-1.522083	1.112925	2.126834
0.012	0.1	-1.4117	0.8458	1.7363	-1.411899	0.848340	1.736122
0.012	0.3	-1.4685	1.0047	1.9424	-1.468555	1.005040	1.942304

fluid has a significant effect on the fluid velocity, temperature distribution and volume fraction of the nanoparticles. Figures 4-6 show how these modifications to the flow field profiles can be described in sense of power law fluid viscosity index n. Steadily rising temperature profile is where the impact of n becomes most apparent. The concentration of nanoparticles in the boundary layer increases gradually as n rises. As n grows larger, the velocity profile flattens out. This is because, for a given value of n, the fluid goes from being shear-thin to shear-thick. As can be seen in Figure 7, the Eckert number Ec has a considerable impact on $\theta(\eta)$. With an increase in the dissipation parameter, frictional heat is generated and absorbed by the fluid. When this occurs, the boundary layer's temperature profile improves. However, the concentration and velocity profiles show little to no change as Ec is varied. If we inspect Figure 8, we can see that the temperature profile rises with value of the heat source parameter δ. However, the concentration profile does not significantly shift as value of the heat source parameter δ is varied.

The effects of nondimensional controlling factors on skin friction, Nusselt, and Sherwood numbers were shown in Table 1. The table shows that increasing the power law index and Weissenberg number boost friction factor while decreasing heat and mass movement rates. Increases in the thermal Grashof number and radiation parameters have a proportionate relationship with the friction factor, heat, and mass transfer rate, but the Hartmann number has an inverse proportional relationship with same physical interest values. Table 1 further shows that as unsteadiness and suction/injection parameters increase, heat and mass transfer rates increase while the coefficient of skin friction decreases. When the heat source parameter is increased, the skin friction coefficient and mass transfer rate increase, but heat transfer rates decrease.

Conclusion

In the present study, we have observed the following outcomes. On increasing the values of the thermal conductivity

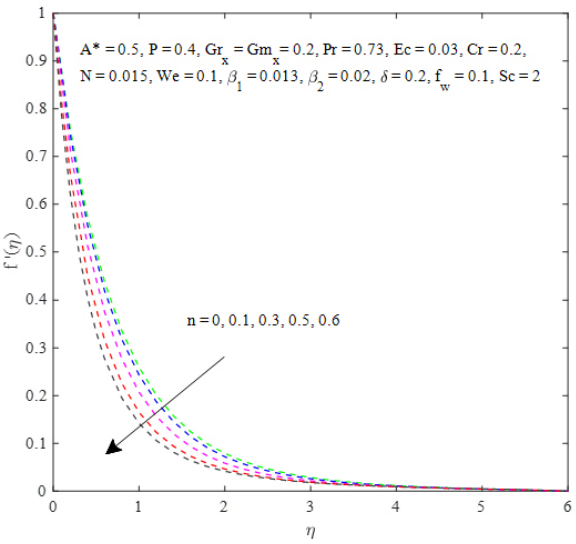

Figure 4: Velocity profile against n

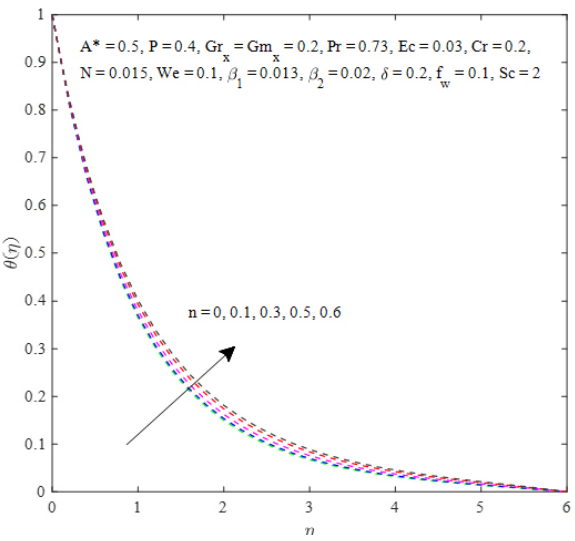

Figure 5: Temperature profile against n

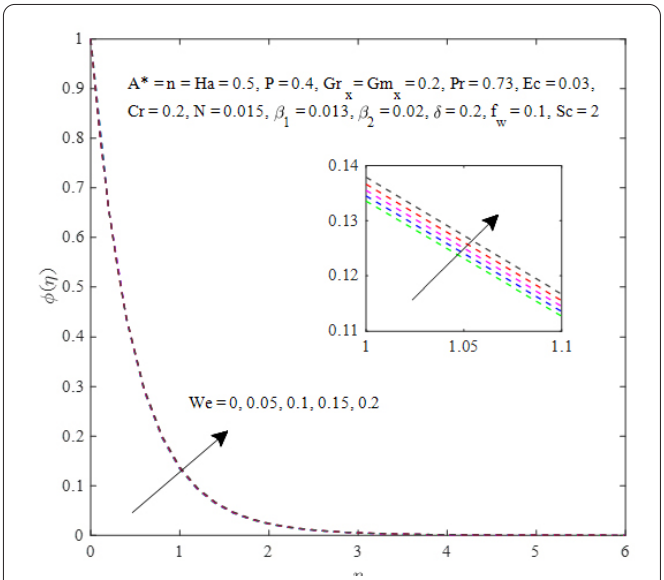

Figure 3: Concentration profile against We.

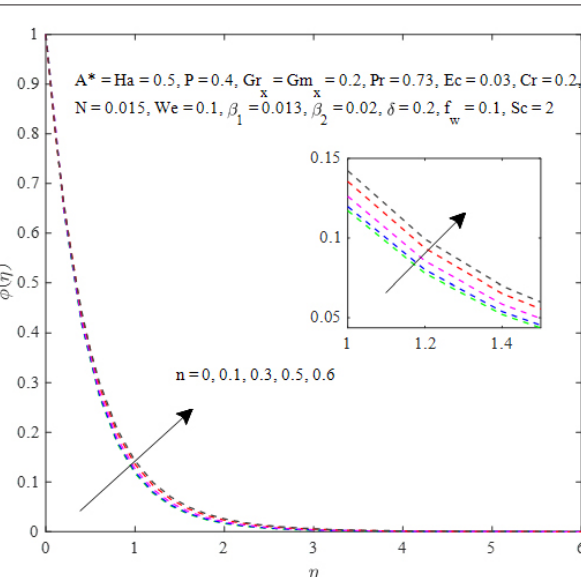

Figure 6: Concentration profile against n.

Table 1: Numerical values of C_{fx}, Nu_x and Sh_x when P= 0.4,Pr=0.73,Ec=0.03,Gm_x=0.2,β_1=0.013,β_2=0.2,Cr=0.2 and Sc=2.

n	We	δ	f_w	A^*	Ha	N	Gr	C_{fx}	Nu_x	Sh_x
0.1	0.1	0.2	0.1	0.5	0.5	0.015	0.2	-1.342540	1.086689	2.167902
0.3	0.1	0.2	0.1	0.5	0.5	0.015	0.2	-1.169454	1.068810	2.146080
0.5	**0.05**	0.2	0.1	0.5	0.5	0.015	0.2	-0.981488	1.046171	2.070111
0.5	**0.20**	0.2	0.1	0.5	0.5	0.015	0.2	-0.917946	1.035631	2.422972
0.5	0.1	**0.1**	0.1	0.5	0.5	0.015	0.2	-0.963284	1.083906	2.111704
0.5	0.1	**0.3**	0.1	0.5	0.5	0.015	0.2	-0.961278	0.999919	2.112914
0.5	0.1	0.2	**-0.5**	0.5	0.5	0.015	0.2	-0.720799	0.879833	1.601203
0.5	0.1	0.2	**0.5**	0.5	0.5	0.015	0.2	-1.171894	1.174872	2.544711
0.5	0.1	0.2	0.1	**0.2**	0.5	0.015	0.2	-0.897328	0.794876	1.832127
0.5	0.1	0.2	0.1	**0.4**	0.5	0.015	0.2	-0.941719	0.969747	2.023318
0.5	0.1	0.2	0.1	0.5	**0.2**	0.015	0.2	-0.890101	1.057535	2.128295
0.5	0.1	0.2	0.1	0.5	**0.4**	0.015	0.2	-0.938900	1.047677	2.117426
0.5	0.1	0.2	0.1	0.5	0.5	**0.053**	0.2	-0.961738	1.064683	2.112631
0.5	0.1	0.2	0.1	0.5	0.5	**0.15**	0.2	-0.960349	1.118312	2.113459
0.5	0.1	0.2	0.1	0.5	0.5	0.015	**0.3**	-0.931460	1.051245	2.120486
0.5	0.1	0.2	0.1	0.5	0.5	0.015	**0.6**	-0.840555	1.073796	2.143525

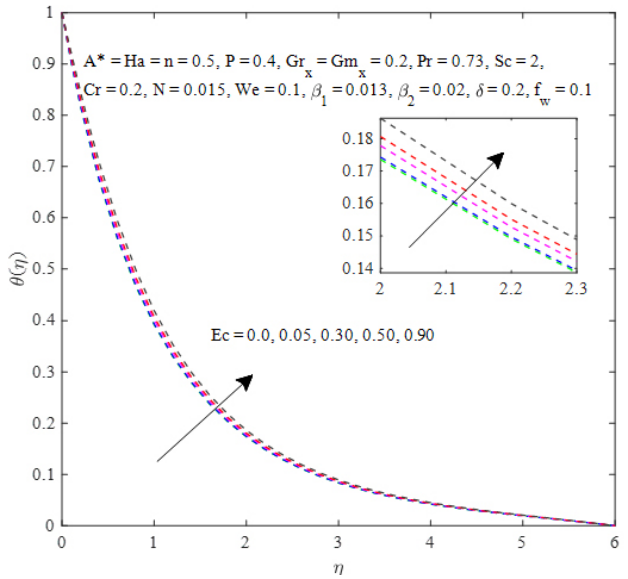

Figure 7: Temperature profile against Ec.

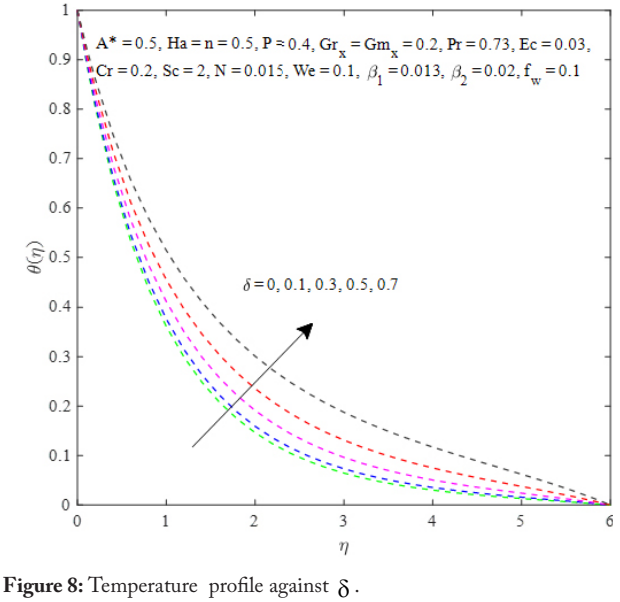

Figure 8: Temperature profile against δ.

and diffusion coefficient, concentration Grashof number, thermal Grashof number, and heat generation/absorption factors results in an increase in velocity. Increasing the power law index, Weissenberg number, Eckert number, thermal radiation, or the heat generation/absorption parameter improves the temperature distribution. Increasing the values of the power law index, the Weissenberg number, and the variable diffusion coefficient will increase the nanoparticle concentration. It is also seen that the combination of porosity and magnetic parameters can decrease the nanofluid velocity, improve the patterns subject to temperature and concentration, and slow down the rates related to mass and heat over the skin. Gains for momentum, heat, and mass transfer rates were demonstrated to result from a rise in thermal radiation, concentration Grashof number, and thermal Grashof number. The skin friction coefficient increases as the heat and mass transfer rates decrease as power law index and Weissenberg number grow larger.

References

1. Hayat T, Shafique M, Tanveer A, Alsaedi A. 2016. Magnetohydrodynamic effects on peristaltic flow of hyperbolic tangent nanofluid with slip conditions and Joule heating in an inclined channel. *Int J Heat Mass Transf* 102: 54–63. https://doi.org/10.1016/j.ijheatmasstransfer.2016.05.105
2. Ibrahim W. 2017. Magnetohydrodynamics (MHD) flow of a tangent hyperbolic fluid with nanoparticles past a stretching sheet with second order slip and convective boundary condition. *Results Phys* 7: 3723-3731. https://doi.org/10.1016/j.rinp.2017.09.041
3. Ullah Z, Zaman G. 2017. Lie group analysis of magnetohydrodynamic tangent hyperbolic fluid flow towards a stretching sheet with slip conditions. *Heliyon* 3(11): e00443. https://doi.org/10.1016/j.heliyon.2017.e00443
4. Khan MI, Qayyum S, Hayat T, Khan MI, Alsaedi A, et al. 2018. Entropy generation in radiative motion of tangent hyperbolic nanofluid in presence of activation energy and nonlinear mixed convection. *Physics Letters A* 382(31): 2017-2026. https://doi.org/10.1016/j.physleta.2018.05.021
5. Ullah Z, Zaman G, Ishak A. 2020. Magnetohydrodynamic tangent hyperbolic fluid flow past a stretching sheet. *Chin J Phys* 66: 258-268. https://doi.org/10.1016/j.cjph.2020.04.011
6. Waqas H, Kafait A, Muhammad T, Farooq U. 2022. Numerical study for bio-convection flow of tangent hyperbolic nanofluid over a Riga plate with activation energy. *Alexandria Engineering Journal* 61(2): 1803-1814. https://doi.org/10.1016/j.aej.2021.06.068
7. ANL/MSD/CP-84938. 1995. Enhancing the thermal conductivity of fluids with nanoparticles, Argonne National Lab, IL, United States.
8. Buongiorno J. 2006. Convective transport in nanofluids. *J Heat Transfer* 128(3): 240-250. https://doi.org/10.1115/1.2150834
9. Hakeem AKA, Ganga B, Ansari SMY, Ganesh NV, Rahman MM. 2017. Nonlinear studies on the effect of non-uniform heat generation/absorption on hydromagnetic flow of nanofluid over a vertical plate. *Nonlinear Analysis: Modelling and Control* 22(1): 1-16. https://doi.org/10.15388/NA.2017.1.1
10. Khan M, Hussain A, Malik MY, Salahuddin T, Khan F. 2017. Boundary layer flow of MHD tangent hyperbolic nanofluid over a stretching sheet: A numerical investigation. *Results in Physics* 7: 2837-2844. https://doi.org/10.1016/j.rinp.2017.07.061
11. Ganesh NV, Kameswaran PK, Hakeem AK, Ganga B. 2019. Second order slip flow of water based nanofluids over a stretching/shrinking sheet embedded in a porous medium with internal heat generation/absorption and thermal jump effects. *Journal of Nanofluids* 8(3): 526-542. https://doi.org/10.1166/jon.2019.1615
12. Kalaivanan R, Ganesh NV, Al-Mdallal QM. 2020. An investigation on Arrhenius activation energy of second grade nanofluid flow with active and passive control of nanomaterials. *Case Studies in Thermal Engineering* 22: 100774. https://doi.org/10.1016/j.csite.2020.100774
13. Kalaivanan R, Ganesh NV, Al-Mdallal QM. 2021. Buoyancy driven flow of a second-grade nanofluid flow taking into account the Arrhenius activation energy and elastic deformation: models and numerical results. *Fluid Dynamics & Materials Processing* 17(2): 319-332. https://doi.org/10.32604/fdmp.2021.012789
14. Makinde OD, Mabood F, Khan WA, Tshehla MS. 2016. MHD flow of a variable viscosity nanofluid over a radially stretching convective surface with radiative heat. *J Mol Liq* 219: 624-630. https://doi.org/10.1016/j.molliq.2016.03.078
15. Ibrahim W, Haq RU. 2016. Magnetohydrodynamic (MHD) stagnation point flow of nanofluid past a stretching sheet with convective boundary condition. *J Braz Soc Mech Sci Eng* 38(4): 1155-1164. https://doi.org/10.1007/s40430-015-0347-z
16. Khan M, Hussain A, Malik MY, Salahuddin T, Khan F. 2017. Boundary layer flow of MHD tangent hyperbolic nanofluid over a stretching sheet: a numerical investigation. *Results Phys* 7: 2837-2844. https://doi.org/10.1016/j.rinp.2017.07.061
17. Saidulu N, Gangaiah T, Lakshmi AV. 2019. Radiation effect on MHD flow of a tangent hyperbolic nanofluid over an inclined exponentially stretching sheet. *International Journal of Fluid Mechanics Research* 46(3): 277-293. https://doi.org/10.1615/InterJFluidMechRes.2018025858
18. Atif SM, Hussain S, Sagheer M. 2019. Effect of viscous dissipation and joule heating on MHD radiative tangent hyperbolic nanofluid with convective and slip conditions. *J Braz Soc Mech Sci Eng* 41: 189. https://doi.org/10.1007/s40430-019-1688-9
19. Oyelakin IS, Lalramneihmawii PC, Mondal S, Nandy SK, Sibanda P. 2020. Thermophysical analysis of three-dimensional magnetohydrodynamic flow of a tangent hyperbolic nanofluid. *Eng Rep* 2(4): e12144. https://doi.org/10.1002/eng2.12144
20. Faisal M, Ahmad I, Javed T. 2021. Dynamics of MHD tangent hyperbolic nanofluid with prescribed thermal conditions, random motion and thermo-migration of nanoparticles. *J Dispers Sci Technol* 1-15. https://doi.org/10.1080/01932691.2021.1931291
21. Prabhakar B, Bandari S, Ul Haq R. 2018. Impact of inclined Lorentz forces on tangent hyperbolic nanofluid flow with zero normal flux of nanoparticles at the stretching sheet. *Neural Comput Appl* 29(10): 805-814. https://doi.org/10.1007/s00521-016-2601-4
22. Mukhopadhyay S. 2013. Slip effects on MHD boundary layer flow over an exponentially stretching sheet with suction/blowing and thermal radiation. *Ain Shams Engineering Journal* 4(3): 485-491. https://doi.org/10.1016/j.asej.2012.10.007
23. Hunegnaw D, Kishan N. 2014. Unsteady MHD heat and mass transfer flow over stretching sheet in porous medium with variable properties considering viscous dissipation and chemical reaction. *Chemical Science International Journal* 4(6): 901–917. https://doi.org/10.9734/ACSJ/2014/11972
24. Vajravelu K, Prasad K, Ng CO. 2013. Unsteady convective boundary layer flow of a viscous fuid at a vertical surface with variable fuid properties. *Nonlinear Anal Real World Appl* 14(1): 455-464. https://doi.org/10.1016/j.nonrwa.2012.07.008
25. Dimian MF, Hadhoda MK. 2004. Natural convection flows with variable viscosity, heat and mass diffusion along a vertical plate. *Mechanics and Mechanical Engineering* 7(2): 61-76.
26. Mjankwi MA, Masanja VG, Mureithi EW, James MN. 2019. Unsteady MHD flow of nanofluid with variable properties over a stretching sheet in the presence of thermal radiation and chemical reaction. *Int J Math Math Sci* 2019: 7392459. https://doi.org/10.1155/2019/7392459